

Quantum control for inhomogeneous broadening compensation in single-photon transducers

Sattwik Deb Mishra*, Rahul Trivedi*, Amir H. Safavi-Naeini, and Jelena Vučković
Ginzton Laboratory, Stanford University, 348 Via Pueblo Mall, Stanford, California 94305, USA

A transducer of single photons between microwave and optical frequencies can be used to realize quantum communication over optical fiber links between distant superconducting quantum computers. A promising scalable approach to constructing such a transducer is to use ensembles of quantum emitters interacting simultaneously with electromagnetic fields at optical and microwave frequencies. However, inhomogeneous broadening in the transition frequencies of the emitters can be detrimental to this collective action. In this article, we utilise a gradient-based optimization strategy to design the temporal shape of the laser field driving the transduction system to mitigate the effects of inhomogeneous broadening. We study the improvement of transduction efficiencies as a function of inhomogeneous broadening in different single-emitter cooperativity regimes and correlate it with a restoration of superradiance effects in the emitter ensembles.

INTRODUCTION

Current superconducting quantum systems are able to achieve non-trivial quantum computational tasks¹ and connecting them as nodes of a quantum internet can realize scalable, distributed quantum computing.² Since superconducting quantum systems operate at microwave frequencies, there are technological restrictions to directly connecting distant systems. Commercial microwave cables are dominated by thermal noise at room temperature and hence cause huge loss over long distances. On the other hand, cryo-cooled superconducting transmission lines are low loss but limited to short distances.³ Optical photons are better ‘flying’ qubits; they can be transmitted with low loss over long distances through optical fibers. To connect superconducting quantum systems, there is a necessity to realize coherent transduction systems that can convert photons coherently and bi-directionally between microwave and optical frequencies.

Many approaches have been proposed to construct such transducers.^{4–5} Microwave-to-optical transducers couple fields oscillating at the respective frequencies through a non-linear medium that can be driven externally to bridge the gap between these frequency regimes. The different types of non-linear media that have been studied so far are, electro-optic materials,^{6–11} magnon modes,^{12–14} optomechanical systems,^{15–29} and broadly, ensembles of atomic systems.^{30–45}

Solid-state emitters (like color centers in diamond and silicon carbide and rare-earth ions doped in crystals) can have transitions coupling to both microwave and optical fields. They provide an attractive platform for implementing transducers owing to the possibility of integration with superconducting quantum systems^{46,47} and scalability afforded by rapidly developing nanofabrication techniques.^{48–50} However, single defects are

often only weakly coupled to the microwave and optical fields, leading to low transduction efficiencies. An approach to overcoming the limitation imposed by such weak couplings is to use ensembles of such emitters coupling to the same microwave and optical channels — the coupling strength is then enhanced by a factor of the number of emitters as a consequence of formation of a collective superradiant state of the emitters.^{51–56}

In practical devices, emitters do not have identical resonant frequencies^{57–59} — this inhomogeneous broadening in the resonant frequencies prohibits the formation of a collective superradiant state and lowers the transduction efficiencies. However, the temporal shape of the lasers driving the emitter ensembles can be experimentally tuned — this opens up the possibility of using quantum control techniques to compensate for inhomogeneous broadening in the emitter ensemble. While quantum control techniques have traditionally been employed to control the state of closed and open quantum systems,^{60,61} in this article we use a time-dependent scattering theory framework⁶² to enable design of quantum controls for single photon scattering and emission from such systems. For the emitter based transduction system, we pose the problem of compensating inhomogeneous broadening as a control problem with respect to the applied laser pulse and use a gradient-based optimization algorithm to demonstrate an order of magnitude improvement in the transduction efficiencies.

RESULTS

The transducer model being considered in this article is schematically depicted in Fig. 1a. The emitter ensemble, with each emitter considered to be a three-level system, is coupled to microwave and optical modes with coupling operators L_μ and L_{opt} respectively, where

$$L_\mu = \sum_{i=1}^N \sqrt{\gamma_\mu} \sigma_\mu^{(i)} \quad \text{and} \quad L_{\text{opt}} = \sum_{i=1}^N \sqrt{\gamma_{\text{opt}}} \sigma_{\text{opt}}^{(i)}. \quad (1)$$

* These authors contributed equally to this work.

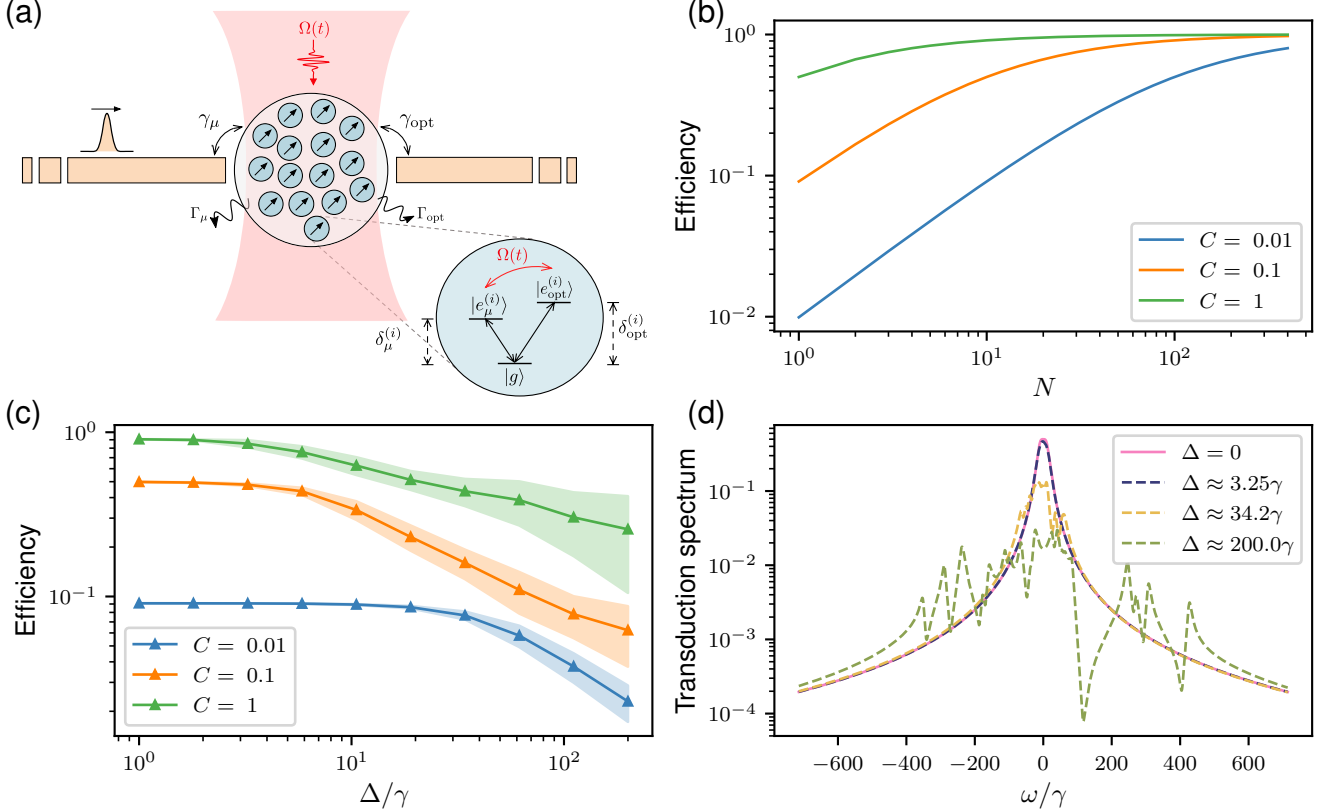


FIG. 1: (a) Schematic of a three-level system ensemble-based transducer device. (b) Scaling of transduction efficiency with increasing number (N) of three-level systems in a homogeneous ensemble for different cooperativities C (we keep γ fixed and vary Γ to vary cooperativity). (c) Decrease in the transduction efficiency through randomly inhomogeneously broadened ensembles of $N = 10$ emitters with increasing inhomogeneous broadening Δ for different cooperativities C . For each value of the inhomogeneous broadening Δ , 100 randomly broadened ensembles are created by sampling the emitter detunings $\delta_\mu^{(i)}, \delta_{\text{opt}}^{(i)}$ from a Gaussian distribution with standard deviation equal to Δ . Each plot point corresponds to the mean over the 100 ensembles with inhomogeneous broadening equal to the corresponding value of Δ and the shaded regions represent the standard deviation. (d) Transduction spectra of ensembles ($N = 10$, $C = 0.1$) with varying inhomogeneous broadening Δ .

Here, γ_μ and γ_{opt} are the decay rates of the emitters into the microwave and optical modes respectively, N is the number of emitters in the ensemble, and $\sigma_\mu^{(i)}$ and $\sigma_{\text{opt}}^{(i)}$ are the lowering operators for transitions of the i th emitter in the ensemble. In addition to coupling to the optical and microwave modes, each emitter can also decay into additional loss channels, modeling unwanted radiative and non-radiative losses, with decay rates Γ_μ and Γ_{opt} from the excited states $|e_\mu^{(i)}\rangle$ and $|e_{\text{opt}}^{(i)}\rangle$, respectively. Furthermore, the transition between the two excited states is driven by a laser with envelope $\Omega(t)$.

For emitter ensembles formed out of identical emitters, the transduction efficiency is determined by the cooperativity of the individual transitions, $C_\mu = \gamma_\mu/\Gamma_\mu$ for microwave and $C_{\text{opt}} = \gamma_{\text{opt}}/\Gamma_{\text{opt}}$ for optical, as well as the number of emitters. We assume $\gamma_\mu = \gamma_{\text{opt}} = \gamma$, $\Gamma_\mu = \Gamma_{\text{opt}} = \Gamma$, and $C_\mu = C_{\text{opt}} = C = \gamma/\Gamma$ in our simulations for simplicity of analysis. Fig. 1b shows the transduction efficiency of this system as a function of the number of

emitters for different emitter cooperativities — due to the formation of a collective superradiant state between the different emitters, this efficiency asymptotically reaches 1 on increasing the number of emitters. Furthermore, the number of emitters needed to obtain high efficiency increases with a decrease in the cooperativity of the individual emitters. We point out that for high microwave and optical cooperativities, near unity transmissions can be obtained with a single emitter and consequently it is unnecessary to use emitter ensembles. We thus focus on low cooperativity emitters in the remainder of this article. On introducing inhomogeneous broadening into the emitter frequencies, the efficiency of the transduction system decreases (Fig. 1c) — for large inhomogeneous broadening, the emitters do not form a collective superradiant mode and the transduction spectrum simply comprises of the individual transduction spectra of the emitters in the ensemble (Fig. 1d).

Since the laser pulse $\Omega(t)$ couples the microwave and optical transitions, we expect that unwanted variations

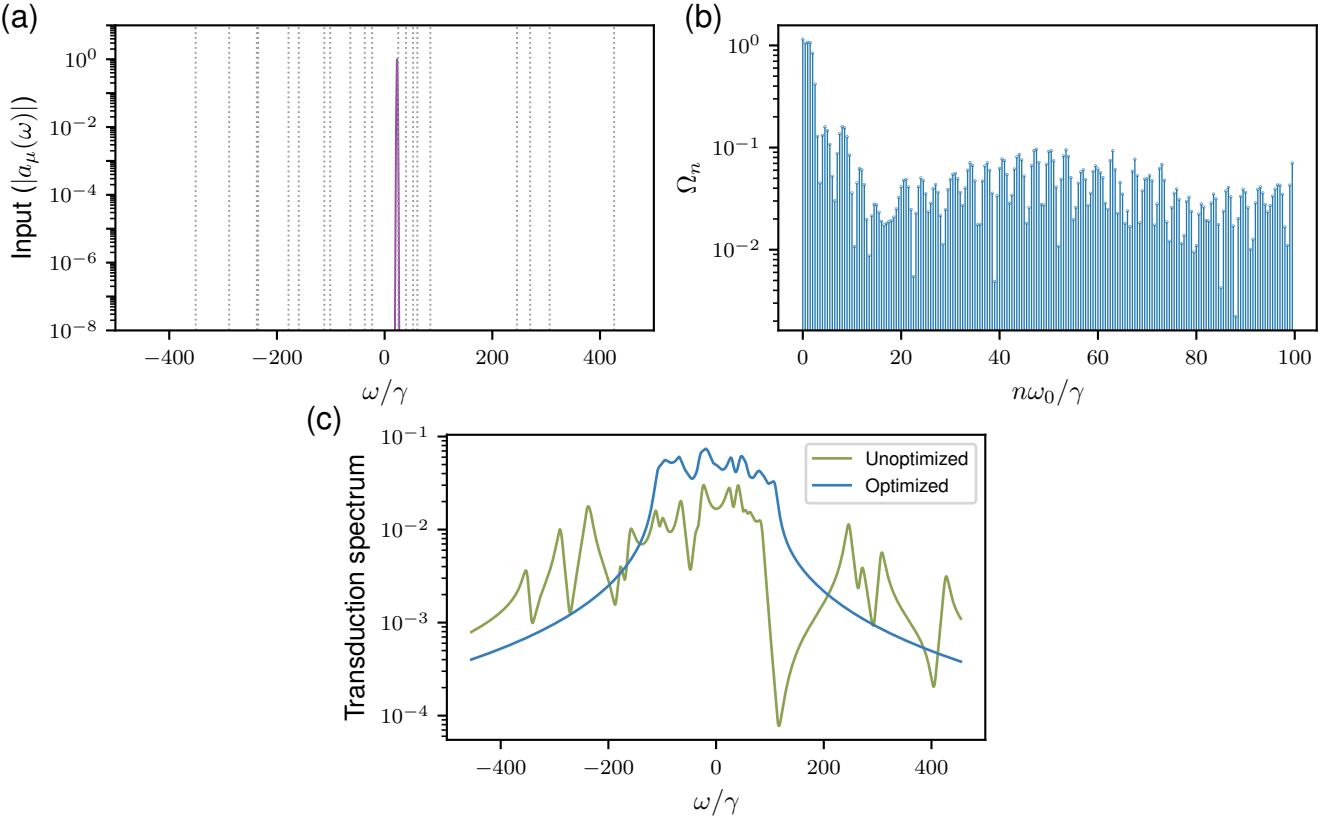


FIG. 2: (a) Fourier transform of the input microwave field (Gaussian waveform). Dashed lines are representative of the individual emitter frequencies in a random ensemble ($N = 10$, $\Delta = 200\gamma$). (b) Amplitudes of the harmonic components of the optimized $\Omega(t)$ designed for the same ensemble. (c) Comparison of the transduction spectrum of the same ensemble with and without optimized drives applied — the transduction spectrum with the optimized drive is computed using a Floquet scattering theory approach.⁶³

in the transition frequencies can be compensated for by modulating the temporal form of this laser. However, in practical transduction systems, it is difficult to address individual emitters with separate lasers and consequently any modulation of $\Omega(t)$ impacts all the emitters. This makes designing the laser pulses difficult and calls for an application of numerical optimization techniques. We thus pose its design as maximizing the total power obtained in the optical mode when the emitter ensemble is excited with a single photon in the microwave mode:

$$\max_{\Omega(t)} \int_{-\infty}^{\infty} dt |a_{\text{opt}}(t)|^2$$

subject to $i \frac{d|\psi_e(t)\rangle}{dt} = H_{\text{eff}}(\Omega(t)) |\psi_e(t)\rangle + a_\mu(t) L_\mu^\dagger |G\rangle$,

$$a_{\text{opt}}(t) = \langle G | L_{\text{opt}} | \psi_e(t) \rangle. \quad (2)$$

where the time-domain wave-packet of the single microwave input photon and optical output photon is described by $a_\mu(t)$ and $a_{\text{opt}}(t)$ respectively, $|\psi_e\rangle$ is the state of the emitters in the ensemble, $|G\rangle$ is the ground state of the ensemble, and $H_{\text{eff}}(\Omega)$ is the non-Hermitian effective Hamiltonian of the system when all the emitters are uni-

formly driven by a laser with amplitude Ω . We point out that the constraints are simply the input-output equations describing the dynamics of the transduction process under excitation with a single photon^{62,64,65} — details of their derivation can be found in the supplementary. Furthermore, since experimentally realizable laser pulses will be band-limited, we parametrize $\Omega(t)$ as a finite sum of harmonics,

$$\Omega(t) = \sum_{n=0}^{N_h} \Omega_n \cos(n\omega_0 t + \phi_n), \quad (3)$$

consequently constraining its bandwidth to be $N_h\omega_0$. The design problem Eq. 2 can be solved using off-the-shelf gradient-based local optimizers. The gradient of the objective function in Eq. 2 with respect to the parameters Ω_n, ϕ_n can be computed using the time domain adjoint-variable method.^{66,67}

As an example, we consider a transduction system with $N = 10$ inhomogeneous emitters excited with a single microwave photon with a Gaussian spectrum. Figure 2a shows the spectrum of the input photon with the dashed lines depicting the resonant frequencies of the transduc-

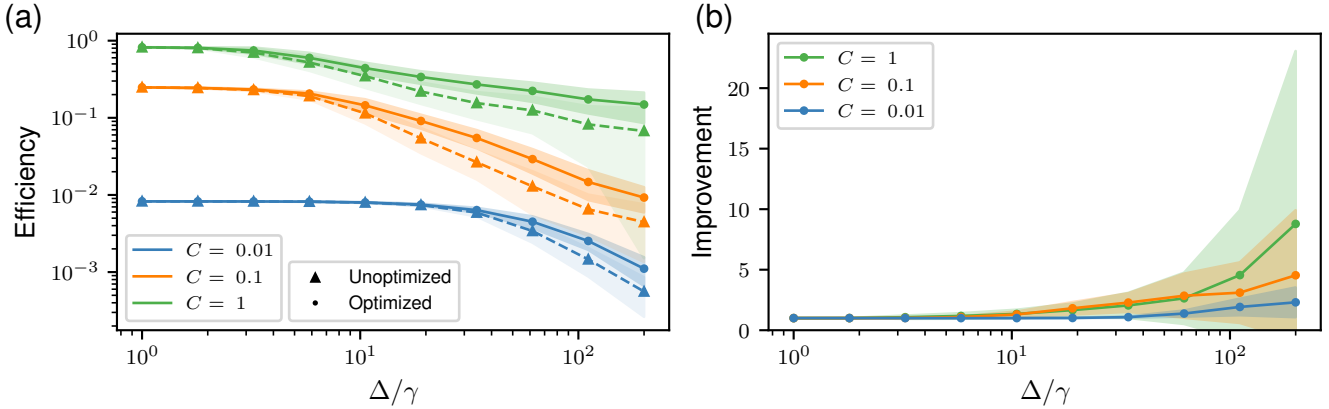


FIG. 3: Optimized drives countering inhomogeneous broadening. (a) Transduction efficiency and (b) improvement in the transduction efficiency through randomly inhomogeneously broadened ensembles of $N = 10$ emitters with increasing inhomogeneous broadening for different cooperativities C when the optimized drives are applied. For each Δ , optimized drives are designed for each of the same 100 randomly generated ensembles with inhomogeneous broadening equal to Δ as used in Fig. 1c. Before running the optimizations, for each ensemble, the input photon is frequency-shifted to match the highest peak of the unoptimized transduction spectrum. Also, the initial condition for the optimization is $\Omega(t) = (N\gamma + \Gamma)/2$, which is a constant drive that maximises the transduction efficiency through a homogeneous ensemble with the same decay rates. Improvement is defined as the ratio of the efficiencies with and without the optimized drive applied. Each plot point corresponds to the mean over the 100 ensembles with inhomogeneous broadening equal to the corresponding value of Δ and the shaded regions represent the standard deviation.

tion spectra of the individual emitters — we note that the input photon effectively only interacts with a single emitter and consequently the transduction efficiency is low. The optimized drive obtained on solving the problem in Eq. 2 is depicted in Fig. 2b — as can be seen from Fig. 2c, the transduction spectrum in the presence of the optimized drive shows improvement relative to the one with constant (unoptimized) drive.

Statistical studies of performance of the optimization procedure for different sets of emitter frequencies is shown in Fig. 3 — Fig. 3a shows the optimized transduction efficiencies and Fig. 3b shows the improvement in the transduction efficiencies. We observe that the improvements are larger at higher inhomogeneous broadening. Furthermore, the cooperativities of the emitters set a limit on improvement that can be obtained by shaping the laser pulse — as can be seen from Fig. 3b, the improvements are generally smaller for lower cooperativities.

While it is intuitively expected that improvement in transduction efficiency with the application of an optimized drive is due to recovery of superradiance, this can be made more concrete by studying the Floquet eigenstates of the optimized (time-dependent) effective Hamiltonian. The ‘superradiance’ in an eigenstate $|\phi\rangle$ can be quantified with the metric,

$$f[|\phi\rangle] = \frac{2}{N\sqrt{\gamma_\mu\gamma_{\text{opt}}}} |\langle G|L_{\text{opt}}|\phi\rangle\langle\phi|L_\mu^\dagger|G\rangle|. \quad (4)$$

For a homogeneous ensemble, the metric is 1 for two eigenstates formed by the drive-induced hybridization of superradiant states corresponding to the microwave and

optical transitions. Furthermore, it is 0 for the remaining eigenstates since they are subradiant/dark. Since the eigenstates for an inhomogeneous ensembles are not perfectly superradiant or subradiant, their corresponding metric lies between 0 and 1 and quantifies the extent of their subradiant or superradiant character. Figure 4a indicates that an application of the optimized drive statistically increases the value of this metric, indicating partial recovery of superradiance. The density plots in Fig. 4(b, c, d) show the distribution of the superradiance metric of the eigenstates of an inhomogeneously broadened ensemble.

The results discussed above indicate that pulse-shaping the laser can be used to improve the performance of transduction systems — however, the optimized laser pulses can only be computed if the emitter frequencies are known. For systems with large number of emitters, such characterization might not be practical at scale and it would be desirable to find an optimized laser pulse which is robust to the specific frequencies of the emitters and depends only on their distribution. In order to design such a laser pulse, we modify the optimization problem in Eq. 2 to

$$\begin{aligned} \max_{\Omega(t)} \quad & \frac{1}{N_s} \sum_{n=1}^{N_s} \int_{-\infty}^{\infty} dt \left| a_{\text{opt}}^{(n)}(t) \right|^2 \\ \text{subject to} \quad & i \frac{d|\psi_e^{(n)}(t)\rangle}{dt} = H_{\text{eff}}^{(n)}(\Omega(t)) |\psi_e^{(n)}(t)\rangle + a_\mu(t) L_\mu^\dagger |G\rangle, \\ & a_{\text{opt}}^{(n)}(t) = \langle G|L_{\text{opt}}|\psi_e^{(n)}(t)\rangle, \end{aligned} \quad (5)$$

where we generate N_s inhomogeneous emitter samples

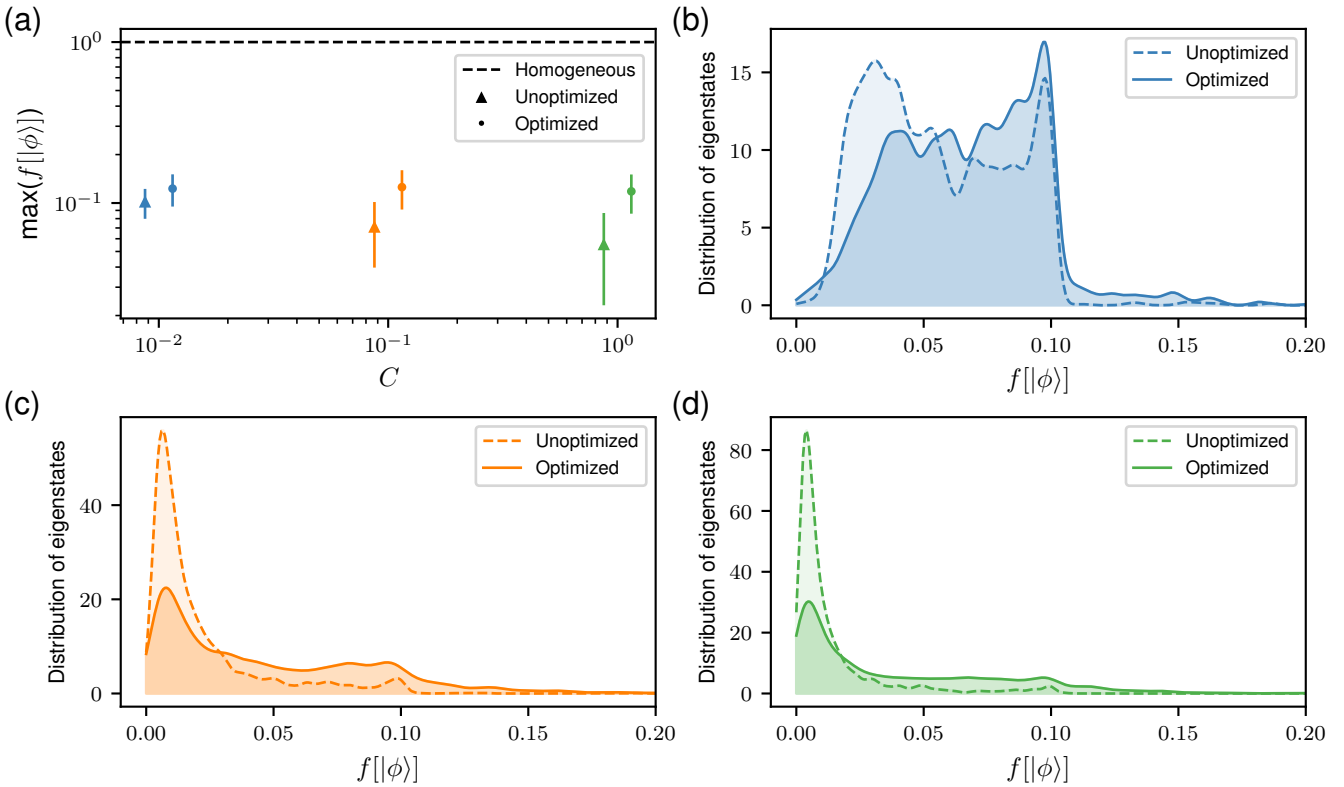


FIG. 4: (a) Comparison of the superradiance metric for ensembles with inhomogeneous broadening $\Delta = 200\gamma$ with and without optimized drives applied (data for optimized and unoptimized cases are dodged in the plot for visual clarity). After generating the optimized drives used in Fig. 3, we compute the metric for all eigenstates of each of the 100 random ensembles with inhomogeneous broadening $\Delta = 200\gamma$ by numerically diagonalising the Floquet operator, i.e., the propagator over one time period of the effective Hamiltonian. Each plot point and associated error bars correspond to the mean and standard deviation (over the collection of ensembles with $\Delta = 200\gamma$) of the maximum value of the superradiance measure $f[|\phi\rangle]$ over all Floquet eigenstates $|\phi\rangle$. The dashed line denotes the same for a homogeneous ensemble. As we increase Γ to decrease the cooperativity, the metric is larger on average in the unoptimized case. We attribute this to the simultaneous increase in the unoptimized drive $\Omega(t) = (N\gamma + \Gamma)/2$ overshadowing the constant inhomogeneous broadening $\Delta = 200\gamma$ (see the supplementary). (b, c, d) Density plots (obtained by kernel density estimation using Gaussian kernels⁶⁸) of the superradiance measure for eigenstates of the 100 ensembles with inhomogeneous broadening $\Delta = 200\gamma$, (b) $C = 0.01$, (c) $C = 0.1$, (d) $C = 1$.

from the same inhomogeneous broadening distribution and find a laser pulse that $\Omega(t)$ that optimizes the average transduced power over all the samples. The superscript over a quantity in Eq. 5 indicates that that quantity is computed for a specific sample. We design such a drive, shown in Fig. 5a, for a training set of $N_s = 100$ random ensembles with inhomogeneous broadening $\Delta = 200\gamma$ and with the input-photon being incident at the resonance of a homogeneous ensemble. Figure 5b shows the resulting improvement in transduction efficiency from applying the optimized drive to a test set of 100 random ensembles that are generated from the same inhomogeneous broadening distribution, independently of the training set. While there is significant improvement over the unoptimized case, we point out that simply shifting the spectrum of the input photon without shaping the driving laser pulse results in similar improvements. Therefore, it is not expected that this optimized drive is restoring superradiance in the emitter ensemble, rather it

is effectively matching the resonance of the transduction spectrum to the input photon in a manner robust to the specific emitter frequencies. This could still be technologically useful since this optimized drive is agnostic to the specific emitter frequencies, thus obviating the need to characterize the emitter resonances. Furthermore, if many transducers are to be operated simultaneously, experimentally realizing and supplying drives customized to each transducer can be challenging to scale — having a common, uncustomized drive would solve this problem.

DISCUSSION

In this article, we have used gradient-based inverse design of the temporal shape of the driving field as a technique to compensate for the effects of inhomogeneous broadening to help realize more efficient transducers. We demonstrated that optimized driving fields can lead to

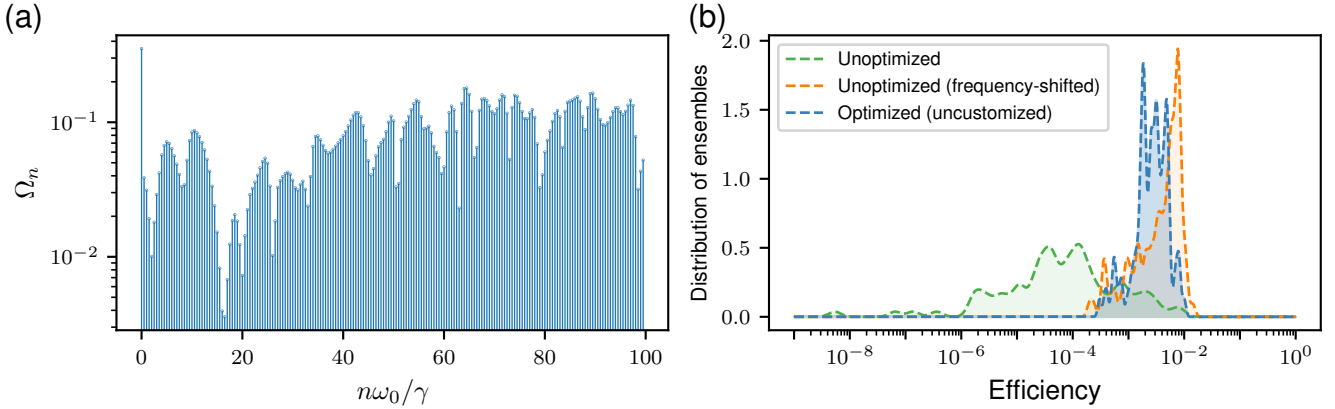


FIG. 5: Transduction efficiency improvement with uncustomized optimization. (a) Amplitudes of the frequency components comprising the uncustomized drive. (b) Density plots of the transduction efficiency through 100 ensembles (test set) with $\Delta = 200\gamma$, $C = 0.1$ for three cases – (green) no optimised drive is applied and the input photon is fixed at the resonance of a homogeneous ensemble, (orange) no optimised drive is applied but the input photon is frequency-shifted to match the highest peak of the unoptimized transduction spectrum for each inhomogeneous ensemble, and (blue) the uncustomized optimized drive is applied and the input photon is fixed at the resonance of a homogeneous ensemble.

improvement in transduction efficiencies and showed that this improvement can be correlated with restoration of superradiant effects.

Our design method is applicable to different physical platforms including color centers or rare-earth ions in solid-state hosts. The techniques used in this article can be extended to ensembles that are orders of magnitude larger by frequency-binning the randomly distributed transition frequencies.⁶⁹ We will explore this direction in future work. In some physical systems the transition frequencies of the emitters can be modulated (for e.g., via Stark effect in V_{Si} centers in SiC). Previous research⁷⁰ has shown that direct modulation of the transition frequencies can also be used to compensate for inhomogeneous broadening in a cavity-QED setting. We anticipate that optimization-based design for transducers can also be applied with the direct modulation as the degree of freedom instead of the driving field.

ACKNOWLEDGEMENTS

This research is funded in part by the U.S. Department of Energy, Office of Science, under Awards DE-SC0019174 and DE-Ac02-76SF00515. R.T. acknowledges funding from Kailath Graduate Fellowship. The authors thank Shuo Sun, Logan Su, Hubert Stokowski, and Kevin Karan Singh Multani for useful discussions.

CONTRIBUTIONS

R.T. and J.V. conceived the idea of using optimisation-based design of drives for inhomogeneous broadening compensation. R.T., S.D.M., and A.H.S.-N. designed the numerical experiments. S.D.M. and R.T. performed the numerical and theoretical analysis. All authors wrote the manuscript.

METHODS

Simulations

We discretize the input-output equations Eq. 2 in time and simulate the dynamics to calculate the transduction efficiency using finite-difference methods. For the customized case, i.e., when the drive is designed for a specific ensemble, we use the L-BFGS-B optimization algorithm. We employ the stochastic optimization algorithm *Adam*⁷¹ to design the uncustomized driving field.

¹ F. Arute, K. Arya, R. Babbush, D. Bacon, J. C. Bardin, R. Barends, R. Biswas, S. Boixo, F. G. S. L. Brandao, D. A. Buell, et al., *Nature* **574**, 505 (2019), ISSN 1476-4687.

² H. J. Kimble, *Nature* **453**, 1023 (2008), ISSN 1476-4687.

³ P. Magnard, S. Storz, P. Kurpiers, J. Schär, F. Marxer, J. Lütolf, J.-C. Besse, M. Gabureac, K. Reuer, A. Akin, et al., arXiv:2008.01642 [quant-ph] (2020), 2008.01642.

⁴ N. J. Lambert, A. Rueda, F. Sedlmeir, and H. G. L. Schwefel, *Advanced Quantum Technologies* **3**, 1900077 (2020), ISSN 2511-9044.

⁵ N. Lauk, N. Sinclair, S. Barzanjeh, J. P. Covey, M. Saffman, M. Spiropulu, and C. Simon, *Quantum Science and Technology* **5**, 020501 (2020), ISSN 2058-9565.

⁶ T. P. McKenna, J. D. Witmer, R. N. Patel, W. Jiang, R. Van Laer, P. Arrangoiz-Arriola, E. A. Wollack, J. F. Herrmann, and A. H. Safavi-Naeini, arXiv:2005.00897 [physics, physics:quant-ph] (2020), comment: 15 pages, 10 figures. First two authors contributed equally to this work, 2005.00897.

⁷ J. Holzgrafe, N. Sinclair, D. Zhu, A. Shams-Ansari, M. Colangelo, Y. Hu, M. Zhang, K. K. Berggren, and M. Lončar, arXiv:2005.00939 [physics, physics:quant-ph] (2020), 2005.00939.

⁸ M. Soltani, M. Zhang, C. Ryan, G. J. Ribeill, C. Wang, and M. Loncar, *Physical Review A* **96**, 043808 (2017).

⁹ M. Tsang, *Physical Review A* **81**, 063837 (2010).

¹⁰ A. Rueda, W. Hease, S. Barzanjeh, and J. M. Fink, *npj Quantum Information* **5**, 1 (2019), ISSN 2056-6387.

¹¹ A. Rueda, F. Sedlmeir, M. C. Collodo, U. Vogl, B. Stiller, G. Schunk, D. V. Strekalov, C. Marquardt, J. M. Fink, O. Painter, et al., *Optica* **3**, 597 (2016), ISSN 2334-2536.

¹² R. Hisatomi, A. Osada, Y. Tabuchi, T. Ishikawa, A. Noguchi, R. Yamazaki, K. Usami, and Y. Nakamura, *Physical Review B* **93**, 174427 (2016).

¹³ J. R. Everts, M. C. Berrington, R. L. Ahlefeldt, and J. J. Longdell, *Physical Review A* **99**, 063830 (2019).

¹⁴ J. Everts, G. G. G. King, N. Lambert, S. Kocsis, S. Rogge, and J. J. Longdell, *Physical Review B* **101**, 214414 (2020), ISSN 2469-9950, 2469-9969, comment: 5 pages, 5 figures, 1911.11311.

¹⁵ C. Zhong, Z. Wang, C. Zou, M. Zhang, X. Han, W. Fu, M. Xu, S. Shankar, M. H. Devoret, H. X. Tang, et al., *Physical Review Letters* **124**, 010511 (2020).

¹⁶ M. Wu, E. Zeuthen, K. C. Balram, and K. Srinivasan, *Physical Review Applied* **13**, 014027 (2020).

¹⁷ H.-K. Lau and A. A. Clerk, *Physical Review Letters* **124**, 103602 (2020), ISSN 0031-9007, 1079-7114, comment: Close to accepted version, 1904.12984.

¹⁸ W. Jiang, C. J. Sarabalis, Y. D. Dahmani, R. N. Patel, F. M. Mayor, T. P. McKenna, R. V. Laer, and A. H. Safavi-Naeini, *Nature Communications* **11**, 1 (2020), ISSN 2041-1723.

¹⁹ M. Forsch, R. Stockill, A. Wallucks, I. Marinković, C. Gärtner, R. A. Norte, F. van Otten, A. Fiore, K. Srinivasan, and S. Gröblacher, *Nature Physics* **16**, 69 (2020), ISSN 1745-2481.

²⁰ G. Arnold, M. Wulf, S. Barzanjeh, E. S. Redchenko, A. Rueda, W. J. Hease, F. Hassani, and J. M. Fink, *Nature Communications* **11**, 4460 (2020), ISSN 2041-1723.

²¹ T. Bagci, A. Simonsen, S. Schmid, L. G. Villanueva, E. Zeuthen, J. Appel, J. M. Taylor, A. Sørensen, K. Usami, A. Schliesser, et al., *Nature* **507**, 81 (2014), ISSN 1476-4687.

²² R. W. Andrews, R. W. Peterson, T. P. Purdy, K. Cicak, R. W. Simmonds, C. A. Regal, and K. W. Lehnert, *Nature Physics* **10**, 321 (2014), ISSN 1745-2481.

²³ Y.-D. Wang and A. A. Clerk, *Physical Review Letters* **108**, 153603 (2012).

²⁴ L. Tian, *Physical Review Letters* **108**, 153604 (2012).

²⁵ J. T. Hill, A. H. Safavi-Naeini, J. Chan, and O. Painter, *Nature Communications* **3**, 1196 (2012), ISSN 2041-1723.

²⁶ S. Barzanjeh, M. Abdi, G. J. Milburn, P. Tombesi, and D. Vitali, *Physical Review Letters* **109**, 130503 (2012).

²⁷ A. H. Safavi-Naeini and O. Painter, *New Journal of Physics* **13**, 013017 (2011), ISSN 1367-2630.

²⁸ L. Tian and H. Wang, *Physical Review A* **82**, 053806 (2010).

²⁹ K. Stannigel, P. Rabl, A. S. Sørensen, P. Zoller, and M. D. Lukin, *Physical Review Letters* **105**, 220501 (2010).

³⁰ J. G. Bartholomew, J. Rochman, T. Xie, J. M. Kindem, A. Ruskuc, I. Craicu, M. Lei, and A. Faraon, *Nature Communications* **11**, 3266 (2020), ISSN 2041-1723, 1912.03671.

³¹ P. S. Barnett and J. J. Longdell, arXiv:2008.10834 [quant-ph] (2020), comment: 10 pages, 7 figures, 2008.10834.

³² S. Welinski, P. J. T. Woodburn, N. Lauk, R. L. Cone, C. Simon, P. Goldner, and C. W. Thiel, *Physical Review Letters* **122**, 247401 (2019).

³³ T. Vogt, C. Gross, J. Han, S. B. Pal, M. Lam, M. Kiffner, and W. Li, *Physical Review A* **99**, 023832 (2019).

³⁴ D. Petrosyan, K. Mølmer, J. Fortágh, and M. Saffman, *New Journal of Physics* **21**, 073033 (2019), ISSN 1367-2630.

³⁵ X. Fernandez-Gonzalvo, S. P. Horvath, Y.-H. Chen, and J. J. Longdell, *Physical Review A* **100**, 033807 (2019).

³⁶ J. P. Covey, A. Sipahigil, and M. Saffman, *Physical Review A* **100**, 012307 (2019).

³⁷ J. Han, T. Vogt, C. Gross, D. Jaksch, M. Kiffner, and W. Li, *Physical Review Letters* **120**, 093201 (2018), ISSN 0031-9007, 1079-7114.

³⁸ B. T. Gard, K. Jacobs, R. McDermott, and M. Saffman, *Physical Review A* **96**, 013833 (2017), ISSN 2469-9926, 2469-9934.

³⁹ M. Kiffner, A. Feizpour, K. T. Kaczmarek, D. Jaksch, and J. Nunn, *New Journal of Physics* **18**, 093030 (2016), ISSN 1367-2630.

⁴⁰ X. Fernandez-Gonzalvo, Y.-H. Chen, C. Yin, S. Rogge, and J. J. Longdell, *Physical Review A* **92**, 062313 (2015).

⁴¹ L. A. Williamson, Y.-H. Chen, and J. J. Longdell, *Physical Review Letters* **113**, 203601 (2014).

⁴² C. O'Brien, N. Lauk, S. Blum, G. Morigi, and M. Fleischhauer, *Physical Review Letters* **113**, 063603 (2014), ISSN 0031-9007, 1079-7114.

⁴³ M. Hafezi, Z. Kim, S. L. Rolston, L. A. Orozco, B. L. Lev, and J. M. Taylor, *Physical Review A* **85**, 020302 (2012), ISSN 1050-2947, 1094-1622.

⁴⁴ J. Verdú, H. Zoubi, C. Koller, J. Majer, H. Ritsch, and J. Schmiedmayer, *Physical Review Letters* **103**, 043603 (2009).

⁴⁵ A. Imamoğlu, *Physical Review Letters* **102**, 083602 (2009).

⁴⁶ X. Zhu, S. Saito, A. Kemp, K. Kakuyanagi, S.-i. Karmoto, H. Nakano, W. J. Munro, Y. Tokura, M. S. Everitt, K. Nemoto, et al., *Nature* **478**, 221 (2011), ISSN 0028-

0836, 1476-4687.

⁴⁷ G. Dold, C. W. Zollitsch, J. O'Sullivan, S. Welinski, A. Ferrier, P. Goldner, S. de Graaf, T. Lindström, and J. J. Morton, *Physical Review Applied* **11**, 054082 (2019).

⁴⁸ C. Dory, D. Vercruyse, K. Y. Yang, N. V. Sapra, A. E. Rugar, S. Sun, D. M. Lukin, A. Y. Piggott, J. L. Zhang, M. Radulaski, et al., *Nature Communications* **10**, 3309 (2019), ISSN 2041-1723.

⁴⁹ D. M. Lukin, C. Dory, M. A. Gidry, K. Y. Yang, S. D. Mishra, R. Trivedi, M. Radulaski, S. Sun, D. Vercruyse, G. H. Ahn, et al., *Nature Photonics* **14**, 330 (2020), ISSN 1749-4893.

⁵⁰ N. H. Wan, T.-J. Lu, K. C. Chen, M. P. Walsh, M. E. Trusheim, L. De Santis, E. A. Bersin, I. B. Harris, S. L. Mouradian, I. R. Christen, et al., *Nature* **583**, 226 (2020), ISSN 1476-4687.

⁵¹ R. H. Dicke, *Physical Review* **93**, 99 (1954).

⁵² M. Gross and S. Haroche, *Physics Reports* **93**, 301 (1982), ISSN 0370-1573.

⁵³ R. Trivedi, M. Radulaski, K. A. Fischer, S. Fan, and J. Vučković, *Physical Review Letters* **122**, 243602 (2019).

⁵⁴ L.-M. Duan, M. D. Lukin, J. I. Cirac, and P. Zoller, *Nature* **414**, 413 (2001), ISSN 1476-4687.

⁵⁵ A. González-Tudela, V. Paulisch, D. E. Chang, H. J. Kimble, and J. I. Cirac, *Physical Review Letters* **115**, 163603 (2015).

⁵⁶ V. Paulisch, M. Perarnau-Llobet, A. González-Tudela, and J. I. Cirac, *Physical Review A* **99**, 043807 (2019).

⁵⁷ R. E. Evans, A. Sipahigil, D. D. Sukachev, A. S. Zibrov, and M. D. Lukin, *Physical Review Applied* **5**, 044010 (2016), ISSN 2331-7019.

⁵⁸ A. M. Dibos, M. Raha, C. M. Phenicie, and J. D. Thompson, *Physical Review Letters* **120**, 243601 (2018), ISSN 0031-9007, 1079-7114.

⁵⁹ T. Zhong, J. M. Kindem, J. G. Bartholomew, J. Rochman, I. Craiciu, V. Verma, S. W. Nam, F. Marsili, M. D. Shaw, A. D. Beyer, et al., *Physical Review Letters* **121**, 183603 (2018), ISSN 0031-9007, 1079-7114.

⁶⁰ D. Dong and I. R. Petersen, *IET Control Theory Applications* **4**, 2651 (2010), ISSN 1751-8652.

⁶¹ C. P. Koch, *Journal of Physics: Condensed Matter* **28**, 213001 (2016), ISSN 0953-8984, 1361-648X.

⁶² R. Trivedi, K. Fischer, S. Xu, S. Fan, and J. Vuckovic, *Physical Review B* **98**, 144112 (2018).

⁶³ R. Trivedi, A. White, S. Fan, and J. Vučković, *Physical Review A* **102**, 033707 (2020).

⁶⁴ E. Rephaeli and S. Fan, *IEEE Journal of Selected Topics in Quantum Electronics* **18**, 1754 (2012), ISSN 1558-4542.

⁶⁵ S. Fan, S. E. Kocabas, and J.-T. Shen, *Physical Review A* **82**, 063821 (2010).

⁶⁶ W. H. Schmidt, in *Large-Scale Scientific Computing*, edited by I. Lirkov, S. Margenov, and J. Waśniewski (Springer, Berlin, Heidelberg, 2006), Lecture Notes in Computer Science, pp. 255–262, ISBN 978-3-540-31995-5.

⁶⁷ M. A. Swillam, M. H. Bakr, and X. Li, *Applied Optics* **46**, 1492 (2007), ISSN 2155-3165.

⁶⁸ D. W. Scott, *Multivariate Density Estimation* (John Wiley & Sons, Ltd, 1992), 1st ed.

⁶⁹ K. Debnath, Y. Zhang, and K. Mølmer, *Physical Review A* **100**, 053821 (2019).

⁷⁰ D. M. Lukin, A. D. White, R. Trivedi, M. A. Gidry, N. Morioka, C. Babin, Ö. O. Soykal, J. Ul-Hassan, N. T. Son, T. Ohshima, et al., *npj Quantum Information* **6**, 1 (2020), ISSN 2056-6387.

⁷¹ D. P. Kingma and J. Ba, arXiv:1412.6980 [cs] (2017), comment: Published as a conference paper at the 3rd International Conference for Learning Representations, San Diego, 2015, 1412.6980.